

Article

Flowering Phenology and Characteristics of Pollen Aeroparticles of *Quercus* Species in Korea

Iereh Kim, Myeong Ja Kwak , Jong Kyu Lee , Yeaji Lim, Sanghee Park, Handong Kim, Keum-Ah Lee and Su Young Woo * 

Department of Environmental Horticulture, University of Seoul, Seoul 02504, Korea; abqlfk@naver.com (I.K.); 016na8349@hanmail.net (M.J.K.); gpl90@naver.com (J.K.L.); oxll2l@naver.com (Y.L.); parksanghee0930@gmail.com (S.P.); blasterkhd92@gmail.com (H.K.); lka830815@gmail.com (K.-A.L.)

* Correspondence: wsy@uos.ac.kr; Tel.: +82-10-3802-5242

Received: 27 January 2020; Accepted: 16 February 2020; Published: 20 February 2020



Abstract: In recent decades, airborne allergens for allergic respiratory diseases have been found to increase significantly by a process of converting coniferous forests into broad-leaved forests in Korea. This study was conducted to evaluate factors, including airborne pollen counts, micromorphology, and flowering phenology, that can affect oak pollen-related allergic symptoms. The catkin of Mongolian oak (*Quercus mongolica* Fisch. ex Ledeb.) showed the most rapidly blooming catkin on Julian day 104 in flower development. Among six species, the last flowering was observed on Julian day 119 in Korean oak (*Quercus dentata* Thunb.). The pollen dispersal was persisted for about 32 days from Julian day 104 to Julian day 136. Airborne pollen was observed about 2 weeks after flowering phase H, the senescence phase. Pollen size varied by species, with the largest from *Q. mongolica* (polar axis length, PL = 31.72 μm , equatorial axis length, EL = 39.05 μm) and the smallest from Jolcham oak (*Quercus serrata* Murray) (PL = 26.47 μm , EL = 32.32 μm). Regarding pollen wall structure, endexine of *Q. dentata* was coarsely laminated or fragmented. The endexine thicknesses of Sawtooth oak (*Quercus acutissima* Carruth.) and *Q. serrata* were thick and stable, whereas Galcham oak (*Quercus aliena* Blume), *Q. mongolica*, and Oriental cork oak (*Quercus variabilis* Blume) had thinner endexines. The area occupied by pollenkitt of *Q. variabilis* was significantly larger than that of *Q. acutissima*. Importantly, *Q. variabilis* had a distinctly thick 17 kDa protein band, a presumed major allergen. Oak species differ in pollen protein composition, and thus there is a possibility that the allergenic activity of pollen proteins vary depending on oak species. This study highlights the fact that native oak species in Korea differ in flowering pattern of male flowers, pollen morphology, and pollen chemical constituents. These discrepancies in flowering and pollen properties imply variable allergic responses to oak pollen from different species.

Keywords: aeroparticles; allergen; phenology; pollen grains; pollenkitt; *Quercus* spp.

1. Introduction

Korea has large forested areas, with about 60% of the country being forest. Oaks (*Quercus* species) are the most common deciduous trees in Korea. *Quercus* species, which account for 48% of the domestic deciduous forests and 24.9% of the total forest area, are widely distributed throughout the country [1]. *Quercus* species select a favorable period to proceed with the formation of leaves and flower buds. Generally, *Quercus* species undergo formation of leaves and flower buds starting in early spring. They overwinter as buds, and flower the following spring [2]. The species of *Quercus* genus are monoecious in that they have both male and female inflorescences in a single tree. There is a long period between pollination and fertilization, and male flowers mature earlier than female flowers [3]. Like other trees with catkins, *Quercus* is pollinated by wind [4]. *Quercus* species can be commonly found in urban forests

of high-density cities such as Seoul [1,5], and some studies have shown that the area of deciduous forests in Korea is increasing [6,7].

On the basis of allergen sensitization tests conducted in the 1980s, 1990s, and 2010s using 31 pollen allergens, reactivity to tree pollen increased from the 1990s to the 2010s [8]. Furthermore, pollen transferred by wind has extremely low pollenkitt (also called pollen coat) in an outer exine layer [9]. The amount of pollenkitt affects dispersal of pollen grains. Pollenkitt keeps other pollen around and makes several pollens become one mass. Pollen lumps, sticky material, are difficult to blow in the wind. Previous studies [10–13] investigated 61 allergenic plant pollens with transmission electron microscopy (TEM) and found that highly allergenic pollens had less pollenkitt.

Global warming has resulted in a global increase in pollen concentrations, an extension in pollen season, and/or the northward range expansion of the habitat of allergenic pollen taxa, leading to an increasing number of pollen allergic diseases worldwide. Consequently, the pollen-related global public health challenge is increasing [14]. The prevalence of chronic respiratory diseases, including allergic rhinitis and asthma, is estimated to be up to 40% in Europe [15,16]. This problem can be further complicated due to their need to consider several factors such as lifestyle and various environmental changes. For example, climate factors change certain signaling systems, consequently affecting production, dispersal patterns, and allergens (as allergenic proteins) of airborne pollens [17,18]. Among tree pollen allergens, those for oak, birch, alder, and pine have shown significantly increased skin reactivity [8]. Pollen emissions of birch and alder are lower than those of other allergenic tree pollens but are more likely to cause allergy [19]. Even though pines produce large amounts of pollen, pine pollen allergy has not been reported [20]. Previous research has demonstrated that oaks produce enormous amounts of pollen, which acts as an allergen. For example, one grain of pollen contains several kinds of proteins, such as “Que a 1” in *Quercus alba* pollen. This is the only protein characterized as an allergy protein in *Quercus* species [21]. “Que a 1” belongs to the pathogenesis-related intracellular protein class 10 (PR-10 protein group) as does “Bet v 1” from *Betula* pollen. Proteins belonging to PR-10 are known to cause allergic disease [22].

More importantly, because of the large number of oak trees, airborne oak pollen is widespread during spring. A skin reactivity test conducted in recent studies revealed a rate of allergic reactivity to *Quercus* pollen of about 14%, the highest rate among native tree species in Korea. Conversely, the response rates in China and Japan were 6.8% and 10.4% lower, respectively, than that of Korea. This high sensitization rate of *Quercus* pollen indicates the importance of research investigating oak pollen allergy [8,15,23]. The density of airborne pollen is highly correlated with prevalence of allergies. Flowering phenology and pollen emission data can be used to identify species with the greatest influence on airborne pollen density. Furthermore, pollen size affects migration speed and dispersal distance.

Most of the phenology or palynology studies conducted with *Quercus* focus on *Q. alba*, *Quercus robur*, or *Quercus ilex*, which are not present in Korea, and may have pollen characteristics that differ from those of trees that do grow in Korea [24–27]. Therefore, this study was conducted to assess the spatial and temporal patterns of flowering phenology in temperate oak species and to evaluate pollen characteristics for the allergenic potential of oak pollens.

2. Materials and Methods

2.1. Study Site and Plant Material

Pollen sampling was conducted in Seoul, located in the middle of the Korean peninsula. Seoul is the capital of the Republic of Korea, and contains 19.4% of the total population of the Republic of Korea. Phenological patterns of male flowers in five oak species (*Quercus acutissima*, *Quercus aliena*, *Quercus dentata*, *Quercus mongolica*, and *Quercus serrata*) were measured in Baebongsan Neighborhood Park, an urban forest surrounded by a residential area, in northeast Seoul (37°34′52.1″ N, 127°03′48.8″

E) (Figure 1). For this investigation, three trees per species (15 trees) with similar diameter at breast height (DBH) and age were selected.

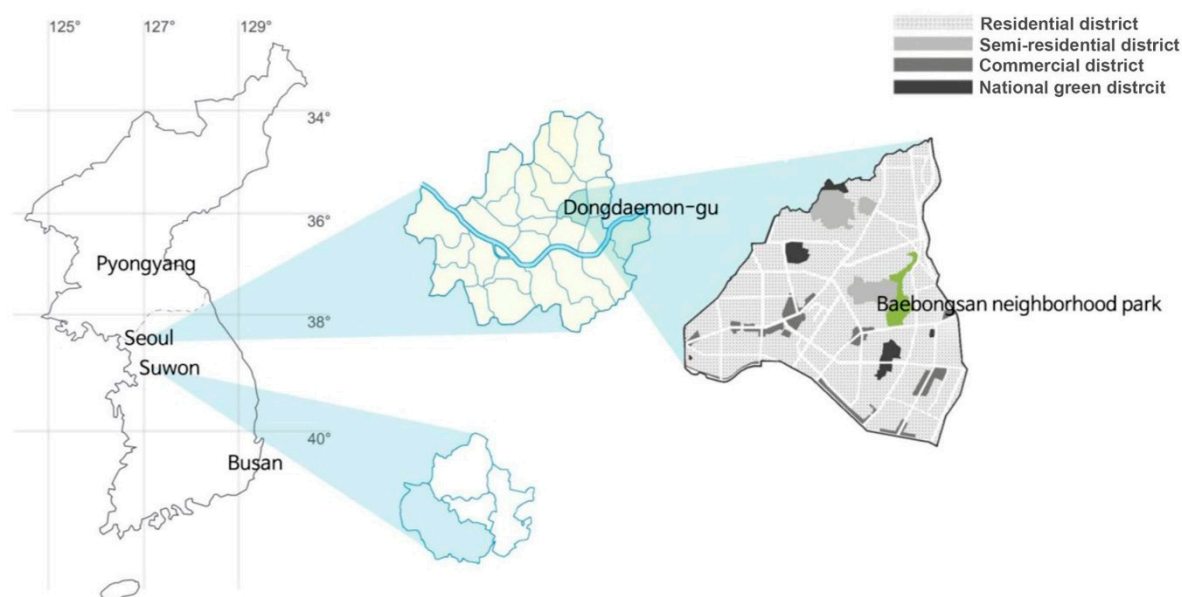


Figure 1. Location of the experimental site (Baebongsan Neighborhood Park and Suwon) and land use of surrounded areas. Baebongsan Neighborhood Park is located in northeast Seoul, Korea, and is surrounded by a residential district.

2.2. Flowering Phenology

Fifteen trees of *Quercus* spp. in Baebongsan Neighborhood Park were selected for this study, and the flowering phenology was monitored six days per week. As shown in Figure 2, detailed descriptions of the flowering stages in male flowers are as follows. (Figure 2A) Winter bud: the first stage of assessment of flowering phenology. Closed buds represent dormancy. The size and shape of buds varied with species, but all were brown. No vegetative green leaves were showing in this stage. (Figure 2B) Bud burst: the bud scale is split, and a new green leaf emerges. (Figure 2C) Catkin development: a green catkin structure appears with its head in an upward position. (Figure 2D) Catkin elongation: the catkin starts to drop, with the head in a downward position. The catkin is still green. (Figure 2E) Maturation of catkin: the catkin is fully elongated, and each male flower separates and lengthens. The flower color changes to yellow green. One or two days pass before the next step, flowering. (Figure 2F) Start of flowering: the first flower of catkin anthesis; most anthers are closed. The flower starts to release pollen at this stage. (Figure 2G) Full flowering: more than 80% of catkins are in anthesis. Almost all flower anthers are in dehiscence. (Figure 2H) Senescence: the catkin turns brown and dries. The flowers stop releasing pollen. (Figure 2I) Catkin falls: flowering is finished, and the dried and twisted catkin falls from the tree.

2.3. Airborne Pollen

The presence and amount of airborne pollen in six oak species (*Quercus acutissima*, *Quercus aliena*, *Quercus dentata*, *Quercus mongolica*, *Quercus serrata*, and *Quercus variabilis*) were measured using a Burkard 7-day recording volumetric trap (Burkard Manufacturing Co. Ltd., Rickmansworth, Hertfordshire, United Kingdom) during the study period. The Burkard spore trap was installed on the roof terrace of a building with 12 m height in Guri, approximately 6 km east of Seoul. Pollen grains were collected daily and counted at 200× magnification with a digital camera (Nikon FDX-35; Nikon, Tokyo, Japan) coupled to a Nikon Labophot-2 microscope.

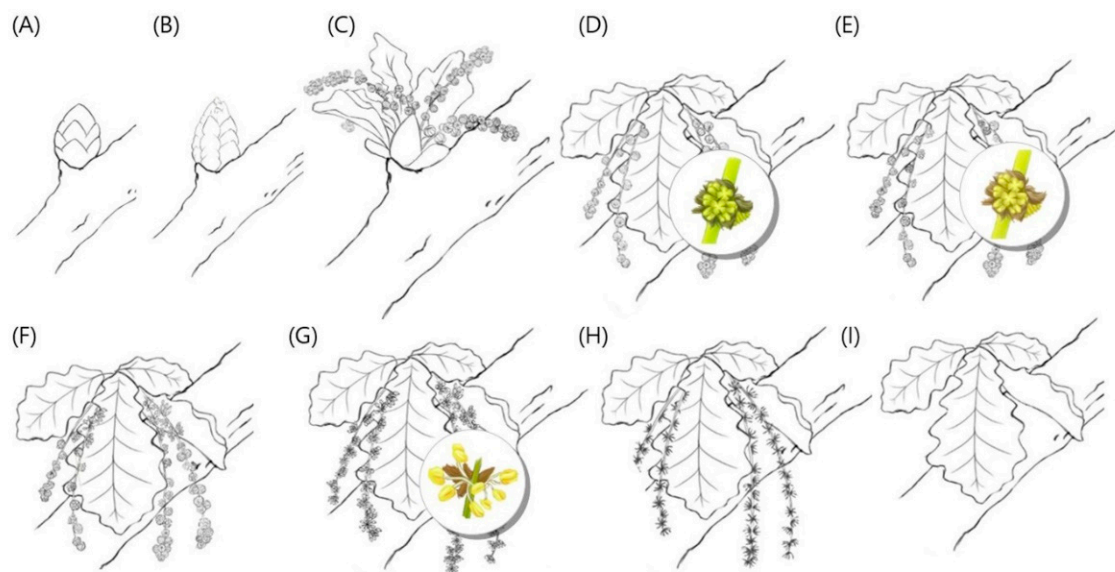


Figure 2. Schematic illustration of nine phenological stages from male flowers of *Quercus* (Fagaceae) in Korea. (A) Winter bud; (B) bud burst; (C) catkin development; (D) catkin elongation; (E) maturation of catkin; (F) start of flowering; (G) full flowering; (H) senescence; (I) catkin fall.

2.4. Size of Pollen Grains

The pollen grains were stained by Calberla's fuchsin staining solution (10 mL of glycerin, 20 mL of 95% alcohol, 30 mL of distilled water, and 0.2 mL of basic fuchsin) [28,29]. The stained pollen grains were viewed and counted under a Nikon Labophot-2 microscope at 400× magnification, and pollen size was measured by the length of polar and equatorial axis defined as follows: polar axis, the maximum diameter of the pollen grains; equatorial axis, the plane perpendicular to the polar axis. At least 100 pollen grains in each *Quercus* species were measured for polar axis length (PL), equatorial axis length (EL), and polar/equatorial length (PL/EL) ratio [30].

2.5. Observation of Pollen Exine Structure

Sections of the pollen wall were observed by TEM. Two milligrams of pollen per species were primarily fixed in modified Karnovsky's fixative [31] overnight in a refrigerator. After fixation, the samples were washed with 0.05 M sodium cacodylate buffer three times. After washing, samples were fixed with 700 µL of 2% OsO₄ and 700 µL of 0.1 M cacodylate buffer for 2 h. The samples were then briefly washed with distilled water twice and stained with 0.5% uranyl acetate overnight. The next day, the samples were dehydrated with ethanol. After transitioning by propylene oxide, samples were infiltrated with propylene oxide and Spurr's resin and polymerized in Spurr's resin for 24 h in a 70 °C dry oven [32]. The sample block was then cut into thin sections of 70–90 nm with a diamond blade in an ultramicrotome and observed with a JEM 1010 (JEOL) TEM at 80 kV [33].

2.6. Soluble Protein Content

Total soluble protein was extracted and quantified by Bradford assay in 1 L of phosphate buffer saline (PBS) composed of 1 L of distilled water, 8 g of NaCl, 0.2 g of KCl, 1.44 g of Na₂HPO₄, 0.24 g of KH₂PO₄, and HCl [34]. Chemicals, except HCl, were dissolved in 900 mL distilled water and stirred on a magnetic stirrer for 2 h. Then, 10 N HCl was added to adjust pH to 7.4 and total solution volume adjusted to 1 L with distilled water. The solution was sterilized by autoclaving at 121 °C for 25 min. Autoclaved PBS was cooled overnight at room temperature. Fifty micrograms of pollen was defatted in 1 mL PBS (1:20 w/v) for 4 h at 4 °C while stirring with a magnetic stirrer. The sample tubes were centrifuged at 14,900× g for 30 min. The supernatant was filtered through a 45 µm Millipore syringe filter and centrifuged again [35]. Dye reagent concentrate (Bio-Rad Protein Assay Kit II) was diluted

with PBS in a 1 to 4 ratio and filtered through an 11 µm Millipore filter (Whatman No. 1 filter). For protein standard, lyophilized bovine serum albumin (Bio-Rad Protein Assay Kit II) was diluted in PBS. Ten micrograms of standard or sample were placed into the microplate well, and 200 µg of dye reagent was added and incubated for at least 5 min. The absorbance values of the sample and standard were measured in a microplate (Bio Tek Instruments, Inc.) at 595 nm.

Solutions for 15% SDS-PAGE resolution and stocking gels were prepared by a protocol modified [36]. Six grams of SDS buffer and 20 g of extracted protein were mixed and warmed at 100 °C for 5 min. After heating, each sample was loaded onto the SDS gel and electrophoresed at 160 V for 70 min. After electrophoresis, the proteins were detected with Coomassie blue staining.

2.7. Statistical Analysis

All statistical analyses were performed using SPSS Statistics 22 software package (SPSS Inc., IBM Company Headquarters, Chicago, IL, USA). Statistically significant differences in size of pollen grains, thickness of endexine, and pollenkitt among *Quercus* species were tested by one-way ANOVA, assessed with Duncan's test ($p < 0.05$).

3. Results

3.1. Flowering Phenology

Q. mongolica showed the earliest bud burst on Julian day 92 (April 1), whereas *Q. acutissima* had the latest bud burst on Julian day 103 (April 12). After bud burst, the catkin of *Q. mongolica* showed the most rapidly blooming catkin on Julian day 104 (phase F, April 13) in flower development. *Q. aliena* bloomed on Julian day 107 (April 16). Two days later, *Q. serrata* flowers bloomed on Julian day 109 (April 18), whereas *Q. acutissima* bloomed on Julian day 111 (April 20). *Q. dentata* was the latest flowering species, blooming on Julian day 119 (April 28). There was a 15-day time lag between onset of *Q. mongolica* and *Q. dentata* flowering phase F. *Q. dentata* showed relatively slow flowering (Figure 3).

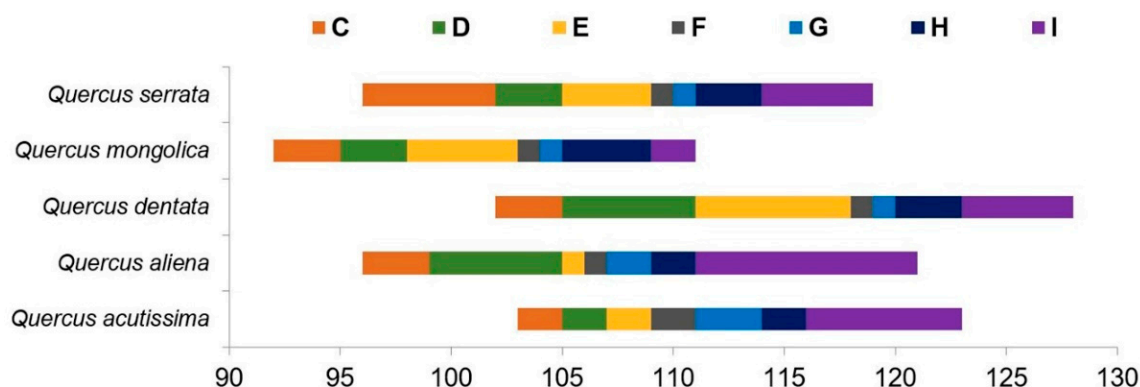


Figure 3. Lengths of flowering stages in oak species (*Quercus acutissima*; *Quercus aliena*; *Quercus dentata*; *Quercus mongolica*; *Quercus serrata*). Abbreviations: (C) catkin development; (D) catkin elongation; (E) maturation of catkin; (F) start of flowering; (G) full flowering; (H) senescence; (I) catkin fall.

The first observation of *Quercus* pollen was on Julian day 104 (April 13) and then was continuously observed until Julian day 136 (May 15). The highest dispersal of airborne pollen into the atmosphere was observed on Julian day 113 (April 22), as indicated in Figure 4. The last observation of *Quercus* flowers was on Julian day 119 (April 28), whereas oak pollen was continuously observed until Julian day 136 (May 15). Airborne pollen was observed about 2 weeks after flowering phase H, the senescence phase.

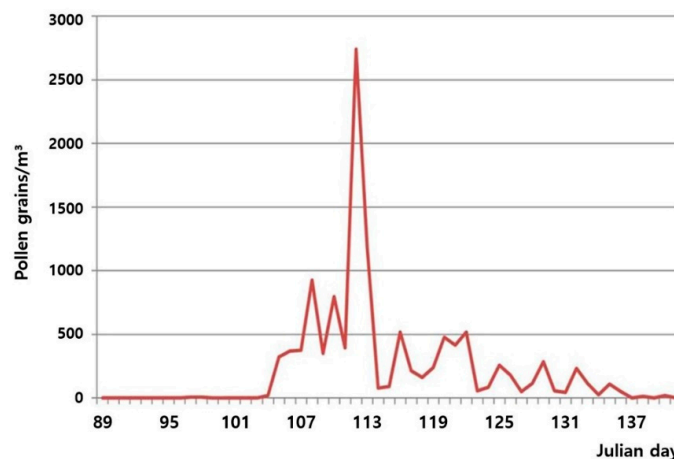


Figure 4. Daily emission of *Quercus* pollen in the spring. The *x*-axis represents the Julian day, and the *y*-axis represents the number of pollen grains collected during the day in the Burkard trap.

3.2. Size of Pollen Grains

The polar and equatorial axes were based on the measurements of at least 100 pollen grains, as detailed in Table 1. Various features of pollen grains were estimated by the following morphometric characteristics: pollen shape, polar axis length (PL), equatorial axis length (EL), and polar/equatorial length (PL/EL) ratio. The shapes of the pollen grains were suboblate, with polar axes ranging from 25.4 to 31.7 μm and equatorial axes ranging from 32.3 to 39.1 μm . Pollen of *Q. mongolica* was bigger than that of other species, with EL and PL of 39.1 μm and 31.7 μm , respectively. The pollen of *Q. acutissima* was the second largest, with an EL of 38.1 μm and PL of 29.6 μm . The pollen sizes of *Q. variabilis*, *Q. dentata*, and *Q. aliena* were similar, with EL values in the range of 33–34 μm . The size of *Q. serrata* pollen was smaller than that of other species, with an EL of 32.3 μm and PL of 26.5 μm . The PL length varied from less than 1 to 7 μm , but there were no significant differences between the two species at $p < 0.001$.

Table 1. Shape and size of *Quercus* pollen grains.

Species	Diameter of Pollen Grain (μm)		PL/EL Ratio	Shape
	EL (μm)	PL (μm)		
<i>Q. acutissima</i>	38.12 ± 2.03^a	29.63 ± 1.64^b	0.78 ^c	Suboblate
<i>Q. aliena</i>	34.37 ± 2.94^b	28.21 ± 1.76^c	0.83 ^b	Suboblate
<i>Q. dentata</i>	34.33 ± 2.14^b	29.01 ± 1.92^b	0.85 ^a	Suboblate
<i>Q. mongolica</i>	39.06 ± 2.35^a	31.72 ± 1.77^a	0.81 ^b	Suboblate
<i>Q. serrata</i>	32.32 ± 1.61^c	26.47 ± 1.11^d	0.82 ^b	Suboblate
<i>Q. variabilis</i>	33.40 ± 1.94^b	25.42 ± 1.83^e	0.76 ^c	Suboblate

Data are presented as the mean \pm standard deviation ($n = 100$). For each of the traits for pollen grain size, different superscripts within columns indicate significant differences among species according to Duncan's test ($p < 0.05$). Abbreviations: EL, equatorial axis length; PL, polar axis length; PL/EL ratio, polar/equatorial length ratio.

The PL/EL ratio was less than 1 in all species. *Q. dentata* pollen had a spherical shape, with a PL/EL ratio of 0.846. *Q. aliena*, *Q. mongolica*, and *Q. serrata* had similar PL/EL ratios. *Q. acutissima* and *Q. variabilis* showed lower PL/EL ratios than other *Quercus* species, and these species had oblate pollen grains. The PL/EL ratio of *Q. dentata* was significantly higher than those of *Q. aliena*, *Q. mongolica*, and *Q. variabilis* at $p < 0.001$.

3.3. Specificity of Pollen Endexine Thickness

Q. mongolica, *Q. aliena*, *Q. variabilis*, *Q. serrata*, and *Q. acutissima* did not show substantial differences in the morphological structure of the pollen exine. Specifically, these species showed exine ultrastructures such as tectum, columellae, and a foot layer. Conversely, the endexine layer of *Q. dentata*

was coarsely laminated or fragmented (Figure 5). There were significant differences in pollen endexine thickness depending on species. Specifically, the endexine thicknesses of *Q. acutissima* and *Q. serrata* were 104.27 μm and 108.96 μm , respectively, which were significantly greater than those of *Q. aliena*, *Q. mongolica*, and *Q. variabilis* at 41.68 μm , 33.41 μm , and 33.17 μm , respectively. The lowest value of *Q. mongolica* was 3.2 times lower than that of *Q. serrata* (Figure 6).

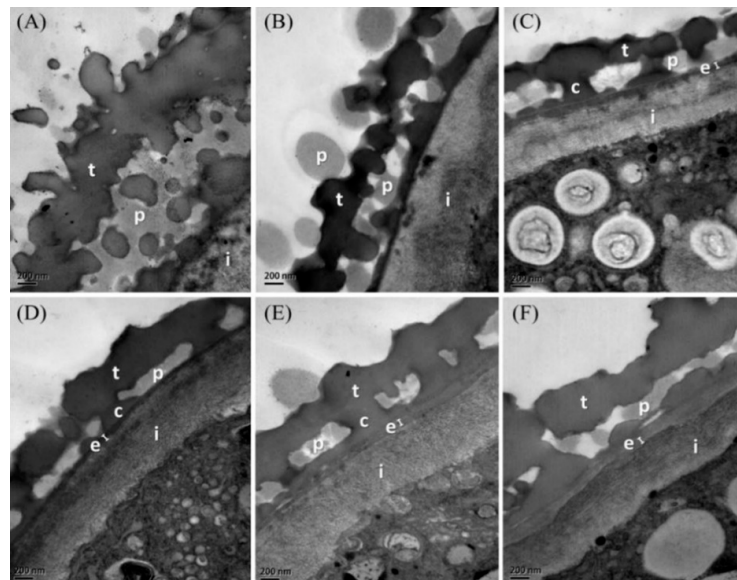


Figure 5. Structure of *Quercus* pollen walls under TEM. (A) *Q. dentata*, (B) *Q. mongolica*, (C) *Q. aliena*, (D) *Q. variabilis*, (E) *Q. serrata*, (F) *Q. acutissima*. Abbreviations: c, collumella; e, endexine; i, intine; p, pollenkitt; t, tectum. Scale bars represent 200 nm.

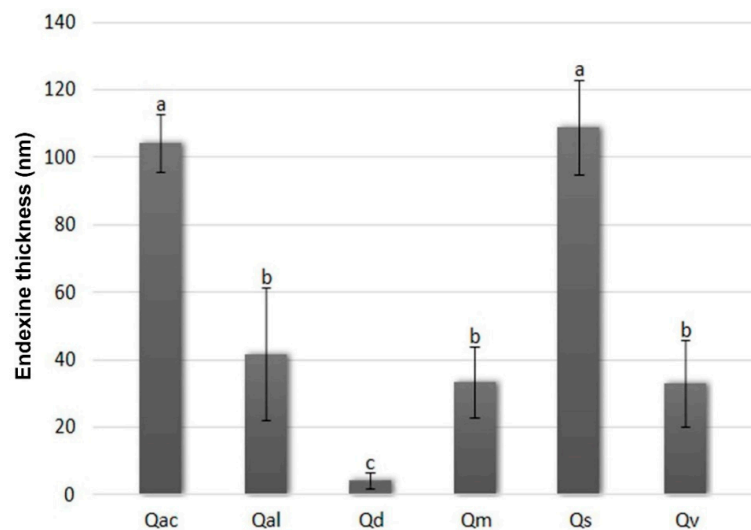


Figure 6. Endexine thickness of oak pollen grains. Abbreviations: Qac, *Q. acutissima*; Qal, *Q. aliena*; Qd, *Q. dentata*; Qm, *Q. mongolica*; Qs, *Q. serrata*; Qv, *Q. variabilis*. Different letters above bars along the x-axis denote statistically significant differences among *Quercus* species at $p < 0.05$.

In the exine layer, the percentage of area occupied by pollenkitt was 98% in *Q. variabilis*. The percentages of pollenkitt in *Q. aliena*, *Q. dentata*, and *Q. mongolica* were 87%, 88%, and 94%, respectively. *Q. variabilis*, *Q. aliena*, *Q. dentata*, and *Q. mongolica* showed different areas of occupation, but the differences were not significant. The percentage of pollenkitt for *Q. serrata* was 79%, whereas that for *Q. acutissima* was 52% (Figure 7). The area occupied by pollenkitt in *Q. variabilis* was significantly larger than that of *Q. serrata* or *Q. acutissima* ($p < 0.05$).

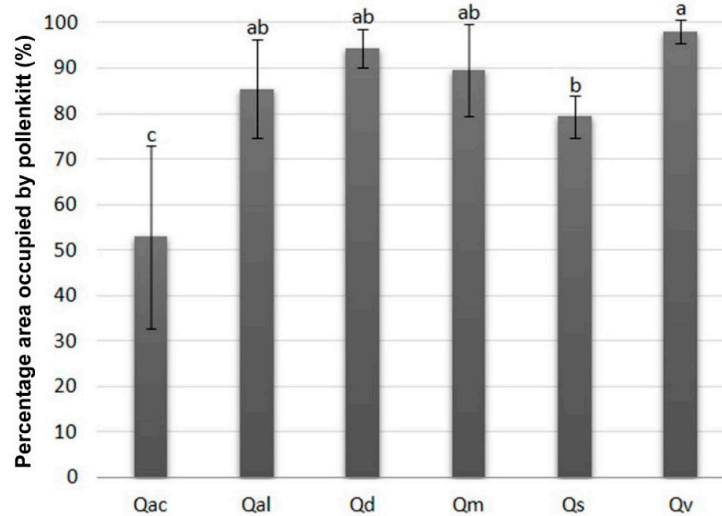


Figure 7. Percentage of occupied area by pollen kitt, the pollen coat covering the outer layer of pollen grains. Abbreviations: Qac, *Q. acutissima*; Qal, *Q. aliena*; Qd, *Q. dentata*; Qm, *Q. mongolica*; Qs, *Q. serrata*; Qv, *Q. variabilis*. Different letters above bars along the x-axis denote statistically significant differences among *Quercus* species at $p < 0.05$.

3.4. Soluble Protein Contents of Pollen

There was no statistically significant difference in soluble protein content among the *Quercus* species. Pollen of *Q. dentata* had a total soluble protein content of $33.51 \mu\text{g}\cdot\text{mL}^{-1}$ (data not shown), highest among the measured values. *Q. mongolica* pollen had $32.39 \mu\text{g}\cdot\text{mL}^{-1}$ of soluble protein, and *Q. serrata* had $31.75 \mu\text{g}\cdot\text{mL}^{-1}$. Pollen of *Q. aliena* and *Q. variabilis* had $31.16 \mu\text{g}\cdot\text{mL}^{-1}$ and $30.16 \mu\text{g}\cdot\text{mL}^{-1}$ total soluble protein, respectively. *Q. acutissima* pollen had the smallest amount of protein, $29.91 \mu\text{g}\cdot\text{mL}^{-1}$. In SDS-PAGE, the positions of the protein bands were similar in the six different *Quercus* species (Figure 8), indicating similar proteins in their pollen. Protein bands with a molecular weight of 17 kDa were found in all *Quercus* species. However, there was a difference in thickness of the protein bands. *Q. variabilis* had a stronger 17 kDa band than other species. The 25 kDa protein band of *Q. acutissima* and *Q. variabilis* was stronger than that of the four other oak species. *Q. acutissima* had a different protein band pattern between 25–35 kDa.

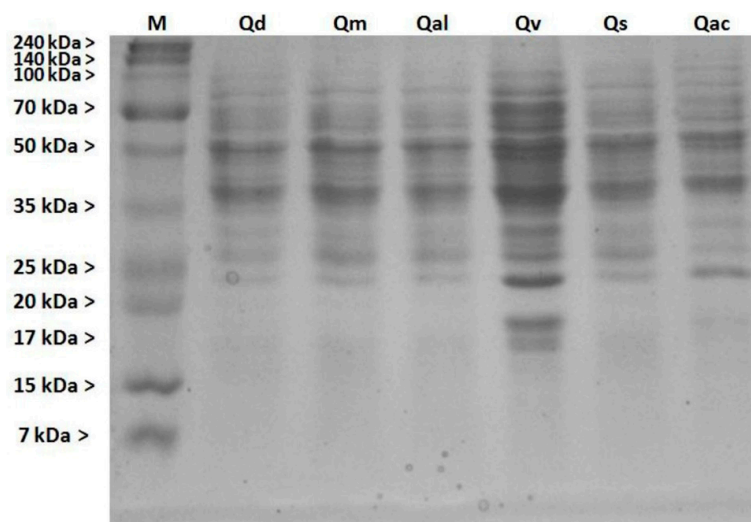


Figure 8. Coomassie blue-stained SDS-PAGE containing protein extracts in *Quercus* pollen. Abbreviations: M, marker; Qd, *Q. dentata*; Qm, *Q. mongolica*; Qal, *Q. aliena*; Qv, *Q. variabilis*; Qs, *Q. serrata*; Qac, *Q. acutissima*.

4. Discussion

Airborne pollen can be dispersed over hundreds (even thousands) of kilometers from the source, causing significant ecological, evolutionary, and clinical effects [37]. Pollen is the most important factor in effective reproduction on plants, but it is also a major cause of seasonal allergy-related diseases (allergic rhinitis, conjunctivitis, bronchial asthma, etc.) and airborne particulate pollutants affecting public health [38]. For allergic patients, the most effective way to prevent allergic reactions is to reduce time spent outside when a large amount of pollen is in the air [39]. For this reason, there have been many studies to develop pollen calendars that indicate dates of high airborne levels of pollen associated with allergies [40–43].

According to [44], the male flower starts to emit pollen from flowering phase F. On the basis of this, it can be assumed that the *Quercus* species that emit pollen at the peak of the pollen season (Julian day 113, April 22) are *Q. serrata*, *Q. aliena*, and *Q. acutissima*. The authors in [45] showed that airborne pollen was observed from the pre-flowering season in *Olea europaea*, and the greatest airborne concentration occurred at the time of flowering. Furthermore, they reported that weather conditions during the pre-flowering season affected the onset of the flowering. Phenological observations conducted in eastern Romania revealed that the length of the male flowering period was about 4 to 6 days in *Quercus* spp., from April 20–25 [46]. Airborne pollen was intensively observed from April 19 to May 5 in a 2009–2010 study conducted in Ulsan, Korea [47]. *Quercus* pollen was present in large amounts for 5 to 6 days in April and May when the florets opened.

Pollen morphology and ultrastructure play a significant role in characterization of the pollen grains. Table 1 shows morphological features of pollen shape, polar axis length (PL), equatorial axis length (EL), and polar/equatorial length (PL/EL) ratio. In a previous study [48], the size of the *Quercus* pollen was about 39 μm , which was larger than the pollen observed in this study. Conversely, another study reported a measure of about 28 μm [30], which was relatively small compared to the present study. In a study of pollen size of *Quercus* in Korea, the mean PL value ranged from 25 to 49 μm , and that of EL was 22 to 39 μm , with very large variation in pollen size (Table 1). In a recent study on *Quercus* pollen emission and transport models, the size of oak pollen was set at 31 μm [49].

Due to the potential distributions of allergenic species with climate change, pollen allergy syndrome will play an important issue for human health in the coming decades [16]. Subdivision of the pollen size of species and further studies will help increase model accuracy. For instance, small and lightweight pollen has the potential for long-distance pollen dispersal, because of aerodynamic behavior such as size, shape, density, and terminal settling velocity, and is a trigger for allergic reactions at a noticeable level [50]. A similar trend has been observed in *Zea mays* [51], where pollen speed ranged from 21 cm/s for pollen grains of 76–80 μm to 32 cm/s for pollen grains of 103–106 μm . In that study, pollen migration speed of *Quercus* was slowest (7.87 cm/s) in *Q. serrata* and fastest (9.47 cm/s) in *Q. mongolica* under no wind. However, factors other than size and weight that affect the velocity of pollen, such as photoperiod, temperature, and pollen density, were not considered. Because of the different sizes of pollen depending on species, pollen dispersal speed and distance will vary by species.

Furthermore, previous studies in pollen dispersal have suggested that pollen transport depends not only on meteorological variations (even pollutants) but also on biological rhythm [52–54]. Despite its lightness, anemochorous pollen is more easily affected by wind than entomophilous pollen. Moreover, the surface of anemochorous pollen grains is relatively smooth compared to that of entomophilous pollen. The pollen grains of wind-pollinated plants have small amounts of pollenkitt in the exine layer, with the amount of pollenkitt affecting the dispersal abilities of the pollen grains [9]. Across previous studies [10–13], there is clear and consistent evidence that high allergenic pollens have relatively less pollenkitt. The stickiness of pollenkitt results in agglomeration of several pollens into one mass [9,11,12,55]. Pollen with a small amount of pollenkitt is more easily affected by wind than that with a large amount. From this point of view, the pollens of *Q. acutissima* and *Q. serrata* can be transported farther than those of *Q. variabilis*, *Q. mongolica*, *Q. dentata*, and *Q. aliena* (Figures 6 and 7).

Normally, pollen structure is supported by a solid outer wall known as the exine. Once airborne pollens are placed in a lipid-rich stigma or encounter rain, the pollen will absorb the medium and swell [56,57]. Furthermore, the proteins in the outer wall or inside the pollen are extremely water-soluble. Thereby, intracellular proteins are released from the pollen through the aperture. An exceptionally thick intine surrounded beneath the exine becomes swollen and ruptured in contact with water, leading to breakdown of the sporopollenin-filled thin exine. Even if the exine is not destroyed, that of swollen pollen is susceptible to damage [58,59]. The exine usually consists of two layers, the outer ectexine and the inner endexine. Previous studies [10,58] showed that the endexine layer of major allergen pollens was not detectable, indicating that it may be easier for the outer wall to break down and release the allergenic protein.

“Que a 1”, with a molecular weight of 17 kDa (Figure 8), is the only identified protein among oak allergens. *Quercus* species are estimated to have several other allergenic proteins; however, the characteristics of each allergenic protein have not been studied. The electrophoresis results showed variability in the appearance of protein bands of *Quercus* spp., indicating differences in pollen proteins depending on species. Furthermore, air pollutant substances such as O₃, NO₂, and CO can affect tree proteins [60]. The effect of atmospheric environment on pollen protein was different by species. Effects of air pollution on *Ostrya carpinifolia*, *Platanus* spp., and *Q. robur* pollen protein were significant. However, there was no significant effect on the pollen grains of *Carpinus betulus* and *Acer negundo* [61,62]. Future studies on the interaction between airborne pollen concentrations and particulate matter on the allergenic potential of pollen proteins are needed. Furthermore, non-uniform spatial conditions such as climatic heterogeneity are strongly linked with pollen production and pollen dispersal patterns, which are known to affect pollen allergenic activity. In particular, oak pollen-related allergic symptoms are concentrated during the dispersal seasons from April to May. Thus, understanding the link between onset and intensity of pollen release and climatic factors is important for public health [63].

5. Conclusions

When the anther starts to dehiscence, pollen is released from the male flower. The pollen of *Quercus* spp. persisted for 32 days in the air, and anther dehiscence occurs in phase F. Airborne pollen was observed about 2 weeks after flowering phase H, the senescence phase. The highest concentration of airborne pollen was from Julian day 111 (April 20) to Julian day 115 (April 24), during which time *Q. serrata*, *Q. aliena*, and *Q. acutissima* emitted large amounts of pollen. The size of *Quercus* spp. ranged from 32 to 38 µm, with significant differences among species. The pollen shape in all investigated *Quercus* species was oblate. Dispersal speed and travel distance of pollen were affected by size. The endexines were thicker in *Q. acutissima* and *Q. serrata* compared with other *Quercus* species. Pollen exines, including endexine, played a role in maintaining the structure of the pollen. When the exine was stable, the pollen was easily disturbed by physical or chemical elements. Notably, intracellular allergy proteins were not easily released. The amount of pollenkit in the pollen exine was small in *Q. acutissima* and *Q. serrata*. Pollen with a small amount of pollenkit did not clump together and may not adhere well to surfaces such as walls or leaves. Therefore, it can be inferred that pollen with large amounts of pollenkit will move further than pollen with small amounts of pollenkit (Figure 9). In electrophoresis of pollen proteins, *Q. variabilis* had the strongest band in 17 kDa, a supposed major allergen, which belongs to the same group with “Que a 1”, the characterized allergy protein in *Q. alba*.

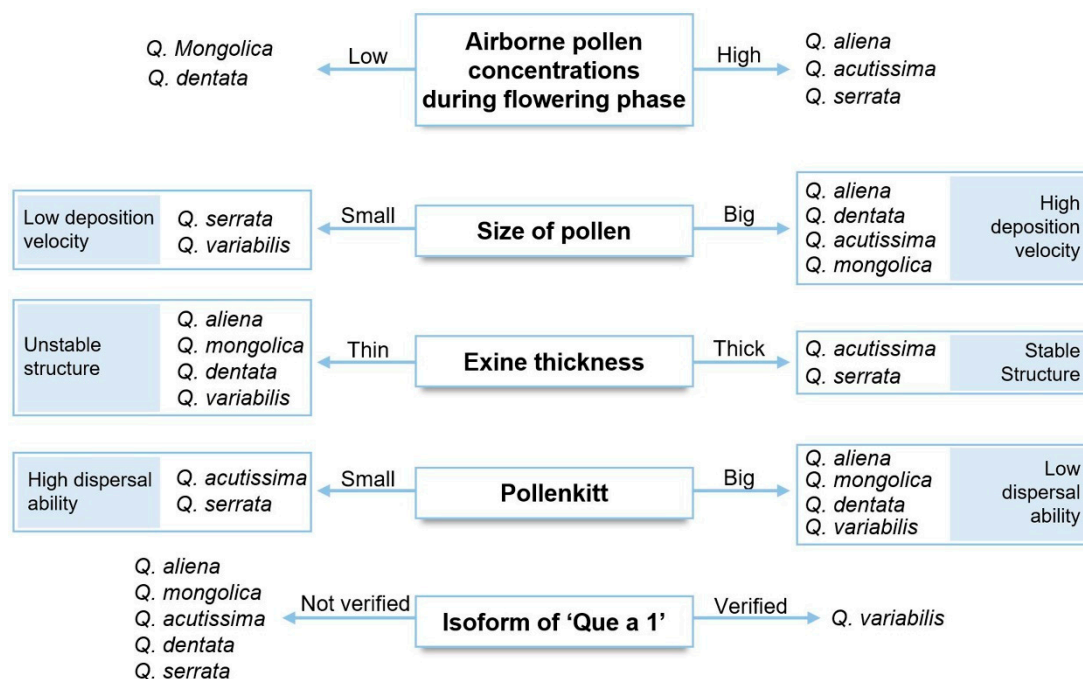


Figure 9. Effects of flowering phenology and pollen characteristics on *Quercus* pollen allergy.

Author Contributions: Conceptualization, S.Y.W.; methodology, I.K.; validation, S.Y.W. and M.J.K.; formal analysis, I.K. and J.K.L.; investigation, Y.L., S.P., and H.K.; resources, K.-A.L.; data curation, I.K.; writing—original draft preparation, I.K.; writing—review and editing, M.J.K.; visualization, M.J.K.; supervision, S.Y.W.; project administration, Y.L.; funding acquisition, S.Y.W. All authors have read and agreed to the published version of the manuscript.

Funding: This work was supported by the Basic Study and Interdisciplinary R&D Foundation Fund of the University of Seoul (2019).

Acknowledgments: This work was supported by the Basic Study and Interdisciplinary R&D Foundation Fund of the University of Seoul (2019).

Conflicts of Interest: The authors declare no conflict of interest. The funders had no role in the design of the study; in the collection, analyses, or interpretation of data; in the writing of the manuscript; or in the decision to publish the results.

References

1. Korea Forest Service. 2019 Statistical Yearbook of Forestry; Korea Forest Service: Daejeon, Korea, 2019; p. 164.
2. Pilar, C.D.; Gabriel, M.M. Phenological pattern of fifteen Mediterranean phanerophytes from shape *Quercus ilex* communities of NE-Spain. *Plant Ecol.* **1998**, *139*, 103–112. [CrossRef]
3. Boavida, L.C.; Silva, J.P.; Feijó, J.A. Sexual reproduction in the cork oak (*Quercus suber* L.). II. Crossing intra-and interspecific barriers. *Sex. Plant Reprod.* **2001**, *14*, 143–152. [CrossRef]
4. Rocheta, M.; Sobral, R.; Magalhães, J.; Amorim, M.I.; Ribeiro, T.; Pinheiro, M.; Conceição Egas, C.; Leonor Morais-Cecílio, L.; Costa, M.M. Comparative transcriptomic analysis of male and female flowers of monoecious *Quercus suber*. *Front. Plant Sci.* **2014**, *5*, 599. [CrossRef] [PubMed]
5. Lee, D.G. *Ecological Management of Forests*; Seoul National University Press: Seoul, Korea, 2012; pp. 179–193.
6. Lee, C.S.; Cho, H.J.; Yi, H. Stand dynamics of introduced black locust (*Robinia pseudoacacia* L.) plantation under different disturbance regimes in Korea. *For. Ecol. Manag.* **2004**, *189*, 281–293. [CrossRef]
7. Kim, H.S.; Lee, S.M.; Song, H.K. Actual vegetation distribution status and ecological succession in the Deogyusan National Park. *Korean J. Environ. Ecol.* **2011**, *5*, 37–46.
8. Park, H.J.; Lim, H.S.; Park, K.H.; Lee, J.H.; Park, J.W.; Hong, C.S. Changes in allergen sensitization over the last 30 years in Korea respiratory allergic patients: A single-center. *Allergy Asthma Immunol. Res.* **2014**, *6*, 434–443. [CrossRef]

9. Edlund, A.F.; Swanson, R.; Preuss, D. Pollen and stigma structure and function: The role of diversity in pollination. *Plant Cell* **2004**, *16*, 84–97. [\[CrossRef\]](#)
10. Diethart, B.; Sam, S.; Weber, M. Walls of allergenic pollen: Special reference to the endexine. *Grana* **2007**, *46*, 164–175. [\[CrossRef\]](#)
11. Culley, T.M.; Weller, S.G.; Sakai, A.K. The evolution of wind pollination in angiosperms. *Trends Ecol. Evol.* **2002**, *17*, 361–369. [\[CrossRef\]](#)
12. Petersen, A.; Dresselhaus, T.; Grobe, K.; Becker, W.M. Proteome analysis of maize pollen for allergy-relevant components. *Proteomics* **2006**, *6*, 6317–6325. [\[CrossRef\]](#)
13. Lin, H.; Gomez, I.; Meredith, J.C. Pollenkitt wetting mechanism enables species-specific tunable pollen adhesion. *Langmuir* **2013**, *29*, 3012–3023. [\[CrossRef\]](#) [\[PubMed\]](#)
14. Ziska, L.H.; Makra, L.; Harry, S.K.; Bruffaerts, N.; Hendrickx, M.; Coates, F.; Saarto, A.; Thibaudon, M.; Oliver, G.; Damialis, A.; et al. Temperature-related changes in airborne allergenic pollen abundance and seasonality across the northern hemisphere: A retrospective data analysis. *Lancet Planet Health* **2019**, *3*, e124–e131. [\[CrossRef\]](#)
15. D’Amato, G.; Cecchi, L.; Bonini, S.; Nunes, C.; Annesi-Maesano, I.; Behrendt, H.; Liccardi, G.; Popov, T.; Van Cauwenberge, P. Allergenic pollen and pollen allergy in Europe. *Allergy* **2007**, *62*, 976–990. [\[CrossRef\]](#) [\[PubMed\]](#)
16. Lake, I.R.; Jones, N.R.; Agnew, M.; Goodess, C.M.; Giorgi, F.; Hamaoui-Laguel, L.; Semenov, M.A.; Solomon, F.; Storkey, J.; Vautard, R.; et al. Climate change and future pollen allergy in Europe. *Environ. Health Perspect.* **2017**, *125*, 385–391. [\[CrossRef\]](#) [\[PubMed\]](#)
17. Singer, B.D.; Ziska, L.H.; Frenz, D.A.; Gebhard, D.E.; Straka, J.G. Increasing Amb a 1 content in common ragweed (*Ambrosia artemisiifolia*) pollen as a function of rising atmospheric CO₂ concentration. *Funct. Plant Biol.* **2005**, *32*, 667–670. [\[CrossRef\]](#)
18. Anenberg, S.C.; Weinberger, K.R.; Roman, H.; Neumann, J.E.; Crimmins, A.; Fann, N.; Martinich, J.; Kinney, P.L. Impacts of oak pollen on allergic asthma in the United States and potential influence of future climate change. *GeoHealth* **2017**, *1*, 80–92. [\[CrossRef\]](#)
19. Yoon, M.G.; Kim, M.; Jin, H.J.; Shin, Y.S.; Park, H.S. Identification of immunoglobulin E binding components of two major tree pollens, birch and alder. *Allergy Asthma Respir. Dis.* **2013**, *1*, 216–220. [\[CrossRef\]](#)
20. Hong, C.S. Pollen allergy plants in Korea. *Allergy Asthma Respir. Dis.* **2015**, *3*, 237–252. [\[CrossRef\]](#)
21. Heath, M.D.; Collis, J.; Batten, T.; Hutchings, J.W.; Swan, N.; Skinner, M.A. Molecular, proteomic and immunological parameters of allergens provide inclusion criteria for new candidates within established grass and tree homologous groups. *World Allergy Organ. J.* **2015**, *8*, 1–11. [\[CrossRef\]](#)
22. Hoffmann-Sommergruber, K. Pathogenesis-related (PR)-proteins identified as allergens. *Biochem. Soc. Trans.* **2002**, *30*, 930–935. [\[CrossRef\]](#)
23. Park, K.J.; Kim, H.; Kim, K.R.; Oh, J.W.; Lee, S.Y.; Choi, Y.J. Characteristics of regional distribution of pollen concentration in Korean Peninsula. *Korean J. Agric. For. Meteorol.* **2008**, *10*, 167–176. [\[CrossRef\]](#)
24. Smouse, P.E.; Dyer, R.J.; Westfall, R.D.; Sork, V.L. Two-generation analysis of pollen flow across a landscape. I. Male gamete heterogeneity among females. *Evolution* **2001**, *55*, 260–271. [\[CrossRef\]](#) [\[PubMed\]](#)
25. Garcia-Mozo, H.; Galán, C.; Aira, M.J.; Belmonte, J.; de la Guardia, C.D.; Fernández, D.; Gutierrez, A.M.; Rodriguez, F.J.; Trigo, M.M.; Dominguez-Vilches, E. Modelling start of oak pollen season in different climatic zones in Spain. *Agric. For. Meteorol.* **2002**, *110*, 247–257. [\[CrossRef\]](#)
26. Panahi, P.; Pourmajidian, M.R.; Pourhashemi, M. Pollen morphology of *Quercus* (subgenus *Quercus*, section *Quercus*) in Iran and its systematic implication. *Acta Soc. Bot. Pol.* **2012**, *81*, 33–41. [\[CrossRef\]](#)
27. Codina, R.; Lockey, R.F. Pollen used to produce allergen extracts. *Ann. Allergy Asthma Immunol.* **2017**, *118*, 148–153. [\[CrossRef\]](#) [\[PubMed\]](#)
28. Solomon, W.R.; Burge, H.R.; Boise, J.R.; Becker, M. Comparative particle recoveries by the retracting rotorod, roto-slide and burkard spore trap sampling in a compact array. *Int. J. Biometeorol.* **1980**, *24*, 107–116. [\[CrossRef\]](#)
29. Park, H.J.; Lee, J.H.; Park, K.H.; Kim, K.R.; Han, M.J.; Choe, H.; Oh, J.W.; Hong, C.S. A six-year study on the changes in airborne pollen counts and skin positivity rates in Korea: 2008–2013. *Yonsei Med. J.* **2016**, *57*, 714–720. [\[CrossRef\]](#)
30. Wrońska-Pilarek, D.; Danielewicz, W.; Bocianowski, J.; Maliński, T.; Janyszek, M. Comparative pollen morphological analysis and its systematic implications on three European Oak (*Quercus* L., Fagaceae) species and their spontaneous hybrids. *PLoS ONE* **2016**, *11*, e0161762. [\[CrossRef\]](#)

31. Morris, J.K. A formaldehyde glutaraldehyde fixative of high osmolality for use in electron microscopy. *J. Cell Biol.* **1965**, *27*, 137–139.
32. Spurr, A.R. A low-viscosity epoxy resin embedding medium for electron microscopy. *J. Ultrastruct Res.* **1969**, *26*, 31–43. [[CrossRef](#)]
33. de Souza, E.H.; Souza, F.V.D.; Rossi, M.L.; Brancalleão, N.; da Silva-Ledo, C.A.; Martinelli, A.P. Viability, storage and ultrastructure analysis of *Aechmea bicolor* (Bromeliaceae) pollen grains, an endemic species to the Atlantic forest. *Euphytica* **2015**, *204*, 13–28. [[CrossRef](#)]
34. Bradford, M.M. A rapid and sensitive method for the quantitation of microgram quantities of protein utilizing the principle of protein-dye binding. *Anal. Biochem.* **1976**, *72*, 248–254. [[CrossRef](#)]
35. Sousa, R.; Duque, L.; Duarte, A.J.; Gomes, C.R.; Ribeiro, H.; Cruz, A.; da Silva, J.C.G.E.; Abreu, I. In vitro exposure of *Acer negundo* pollen to atmospheric levels of SO₂ and NO₂: Effects on allergenicity and germination. *Environ. Sci. Technol.* **2012**, *46*, 2406–2412. [[CrossRef](#)] [[PubMed](#)]
36. Harlow, E.D.; Lane, D. *A Laboratory Manual New York: Cold Spring Harbor Laboratory*; Cold Spring Harbor Laboratory Press: New York, NY, USA, 1998; p. 579.
37. Bogawski, P.; Borycka, K.; Grewling, L.; Kasprzyk, I. Detecting distant sources of airborne pollen for Poland: Integrating back-trajectory and dispersion modelling with a satellite-based phenology. *Sci. Total Environ.* **2019**, *689*, 109–125. [[CrossRef](#)]
38. McInnes, R.N. Pollen, Allergens, and Human Health. In *Oxford Research Encyclopedia of Environmental Science*; Oxford University Press: Oxford, UK, 2019; pp. 1–38.
39. Scialla, T.; Wanner, A. Fundamentals of Asthma Treatment. *Pulmão RJ* **2012**, *21*, 33–40.
40. Lo, F.; Bitz, C.M.; Battisti, D.S.; Hess, J.J. Pollen calendars and maps of allergenic pollen in North America. *Aerobiologia* **2019**, *35*, 613–633. [[CrossRef](#)]
41. McInnes, R.N.; Hemming, D.; Burgess, P.; Lyndsay, D.; Osborne, N.J.; Skjøth, C.A.; Thomas, S.; Vardoulakis, S. Mapping allergenic pollen vegetation in UK to study environmental exposure and human health. *Sci. Total Environ.* **2017**, *599*, 483–499. [[CrossRef](#)]
42. Oh, J.W.; Lee, H.B.; Kang, I.J.; Kim, S.W.; Park, K.S.; Kook, M.H.; Kim, B.S.; Baek, H.S.; Kim, J.H.; Lee, D.J.; et al. The revised edition of Korean calendar for allergenic pollens. *Allergy Asthma Immunol. Res.* **2012**, *4*, 5–11. [[CrossRef](#)]
43. Camacho, I.C. Airborne pollen in Funchal city, (Madeira Island, Portugal)-first pollinic calendar and allergic risk assessment. *Ann. Agric. Environ. Med.* **2015**, *22*, 608–613. [[CrossRef](#)]
44. Gómez-Casero, M.T.; Galán, C.; Domínguez-Vilches, E. Flowering phenology of Mediterranean *Quercus* species in different locations (Córdoba, SW Iberian Peninsula). *Acta Bot. Malac.* **2007**, *32*, 127–146.
45. Aguilera, F.; Valenzuela, L.R. Study of the floral phenology of *Olea europaea* L. in Jaén province (SE Spain) and its relation with pollen emission. *Aerobiologia* **2009**, *25*, 217–225. [[CrossRef](#)]
46. Chesnoiu, E.N.; Șofletea, N.; Curtu, A.L.; Toader, A.; Radu, R.; Enescu, M. Bud burst and flowering phenology in a mixed oak forest from Eastern Romania. *Ann. For. Res.* **2009**, *52*, 199–206.
47. Choi, S.H.; Jung, I.Y.; Kim, D.Y.; Kim, Y.H.; Lee, J.H.; Oh, I.B.; Choi, K.R. Seasonal distribution of airborne pollen in Ulsan, Korea in 2009–2010. *Korean J. Environ. Ecol.* **2011**, *34*, 371–379. [[CrossRef](#)]
48. Moon, H.K.; Kong, M.J.; Song, J.H.; Kim, S.Y.; Kim, J.S.; Jung, E.H.; Park, C.H.; Lee, B.Y.; Hong, S.P. Morphological characteristics of major airborne pollen in Korea peninsula. *J. Species Res.* **2015**, *4*, 159–168. [[CrossRef](#)]
49. Lim, Y.K.; Kim, K.R.; Cho, C.; Kim, M.; Choi, H.S.; Han, M.J.; Oh, I.B.; Kim, B.J. Development of a Oak Pollen Emission and Transport Modeling Framework in Korea. *Atmosphere* **2015**, *25*, 221–233. [[CrossRef](#)]
50. Celenk, S. Detection of reactive allergens in long-distance transported pollen grains: Evidence from Ambrosia. *Atmos. Environ.* **2019**, *209*, 212–219. [[CrossRef](#)]
51. Aylor, D.E. Settling speed of corn (*Zea mays*) pollen. *J. Aerosol. Sci.* **2002**, *33*, 1601–1607. [[CrossRef](#)]
52. Tseng, Y.T.; Kawashima, S.; Kobayashi, S.; Takeuchi, S.; Nakamura, K. Forecasting the seasonal pollen index by using a hidden Markov model combining meteorological and biological factors. *Sci. Total Environ.* **2020**, *698*, 134246. [[CrossRef](#)]
53. Tseng, Y.T.; Kawashima, S. Applying a pollen forecast algorithm to the Swiss Alps clarifies the influence of topography on spatial representativeness of airborne pollen data. *Atmos. Environ.* **2019**, *212*, 153–162. [[CrossRef](#)]

54. Williams, C.G. How meso-scale pollen dispersal and its gene flow shape gene conservation decisions. *New For.* **2017**, *48*, 217–224. [[CrossRef](#)]
55. Oteros, J.; Bartusel, E.; Alessandrini, F.; Núñez, A.; Moreno, D.A.; Behrendt, H.; Schmidt-Weber, C.; Traidl-Hoffmann, C.; Buters, J. *Artemisia* pollen is the main vector for airborne endotoxin. *J. Allergy Clin. Immunol.* **2019**, *143*, 369–377. [[CrossRef](#)] [[PubMed](#)]
56. Traidl-Hoffmann, C.; Kasche, A.; Menzel, A.; Jakob, T.; Thiel, M.; Ring, J.; Behrendt, H. Impact of pollen on human health: More than allergen carriers? *Int. Arch. Allergy Immunol.* **2003**, *131*, 1–13. [[CrossRef](#)] [[PubMed](#)]
57. Wang, Q.; Nakamura, S.; Lu, S.; Xiu, G.; Nakajima, D.; Suzuki, M.; Sakamoto, K.; Miwa, M. Release behavior of small sized daughter allergens from *Cryptomeria japonica* pollen grains during urban rainfall event. *Aerobiologia* **2012**, *28*, 71–81. [[CrossRef](#)]
58. Dahl, Å. Pollen lipids can play a role in allergic airway inflammation. *Front. Immunol.* **2018**, *9*, 2816. [[CrossRef](#)]
59. Visez, N.; Chassard, G.; Azarkan, N.; Naas, O.; Sénéchal, H.; Sutra, J.P.; Poncet, P.; Choël, M. Wind-induced mechanical rupture of birch pollen: Potential implications for allergen dispersal. *J. Aerosol. Sci.* **2015**, *89*, 77–84. [[CrossRef](#)]
60. Silva, M.; Ribeiro, H.; Abreu, I.; Cruz, A.; da Silva, J.E. Effects of CO₂ on *Acer negundo* pollen fertility, protein content, allergenic properties, and carbohydrates. *Environ. Sci. Pollut. Res.* **2015**, *22*, 6904–6911. [[CrossRef](#)]
61. Ribeiro, H.; Duque, L.; Sousa, R.; Abreu, I. Ozone effects on soluble protein content of *Acer negundo*, *Quercus robur* and *Platanus* spp. pollen. *Aerobiologia* **2013**, *29*, 443–447. [[CrossRef](#)]
62. Cuinica, L.G.; Abreu, I.; da Silva, J.C.E. In vitro exposure of *Ostrya carpinifolia* and *Carpinus betulus* pollen to atmospheric levels of CO, O₃, and SO₂. *Environ. Sci. Pollut. Res.* **2014**, *21*, 2256–2262. [[CrossRef](#)]
63. Toro, R.; Córdova, A.; Canales, M.; Mardones, P. Trends and threshold exceedances analysis of airborne pollen concentrations in Metropolitan Santiago Chile. *PLoS ONE* **2015**, *10*, e0123077. [[CrossRef](#)]



© 2020 by the authors. Licensee MDPI, Basel, Switzerland. This article is an open access article distributed under the terms and conditions of the Creative Commons Attribution (CC BY) license (<http://creativecommons.org/licenses/by/4.0/>).